Constraint on the Matter-Antimatter Symmetry-Violating Phase in Neutrino Oscillations

K. Abe,[55] R. Akutsu,[56] A. Ali,[32] C. Alt,[11] C. Andreopoulos,[53, 34] L. Anthony,[34] M. Antonova,[19] S. Aoki,[31] A. Ariga,[2] Y. Asada,[68] Y. Ashida,[32] E.T. Atkin,[21] Y. Awataguchi,[58] S. Ban,[32] M. Barbi,[45] G.J. Barker,[65] G. Barr,[42] C. Barry,[34] M. Batkiewicz-Kwasniak,[15] A. Beloshapkin,[26] F. Bench,[34] V. Berardi,[22] S. Berkman,[4, 61] L. Berns,[57] S. Bhadra,[69] S. Bienstock,[52] A. Blondel,[13, *] S. Bolognesi,[6] B. Bourguille,[18] S.B. Boyd,[65] D. Brailsford,[33] A. Bravar,[13] D. Bravo Berguño,[1] C. Bronner,[55] A. Bubak,[50] M. Buizza Avanzini,[10] J. Calcutt,[36] T. Campbell,[7] S. Cao,[16] S.L. Cartwright,[49] M.G. Catanesi,[22] A. Cervera,[19] A. Chappell,[65] C. Checchia,[24] D. Cherdack,[17] N. Chikuma,[54] G. Christodoulou,[12] J. Coleman,[34] G. Collazuol,[24] L. Cook,[42, 28] D. Coplowe,[42] A. Cudd,[36] A. Dabrowska,[15] G. De Rosa,[23] T. Dealtry,[33] P.F. Denner,[65] S.R. Dennis,[34] C. Densham,[53] F. Di Lodovico,[30] N. Dokania,[39] S. Dolan,[12] O. Drapier,[10] J. Dumarchez,[52] P. Dunne,[21] L. Eklund,[14] S. Emery-Schrenk,[6] A. Ereditato,[2] P. Fernandez,[19] T. Feusels,[4, 61] A.J. Finch,[33] G.A. Fiorentini,[69] G. Fiorillo,[23] C. Francois,[2] M. Friend,[16, †] Y. Fujii,[16, †] R. Fujita,[54] D. Fukuda,[40] R. Fukuda,[59] Y. Fukuda,[37] K. Gameil,[4, 61] C. Giganti,[52] T. Golan,[67] M. Gonin,[10] A. Gorin,[26] M. Guigue,[52] D.R. Hadley,[65] J.T. Haigh,[65] P. Hamacher-Baumann,[48] M. Hartz,[61, 28] T. Hasegawa,[16, †] N.C. Hastings,[16] T. Hayashino,[32] Y. Hayato,[55, 28] A. Hiramoto,[32] M. Hogan,[8] J. Holeczek,[50] N.T. Hong Van,[20, 27] F. Iacob,[24] A.K. Ichikawa,[32] M. Ikeda,[55] T. Ishida,[16, †] T. Ishii,[16, †] M. Ishitsuka,[59] K. Iwamoto,[54] A. Izmaylov,[19, 26] B. Jamieson,[66] S.J. Jenkins,[49] C. Jesús-Valls,[18] M. Jiang,[32] S. Johnson,[7] P. Jonsson,[21] C.K. Jung,[39, ‡] M. Kabirnezhad,[42] A.C. Kaboth,[47, 53] T. Kajita,[56, ‡] H. Kakuno,[58] J. Kameda,[55] D. Karlen,[62, 61] S.P. Kasetti,[35] Y. Kataoka,[55] T. Katori,[30] Y. Kato,[55] E. Kearns,[3, 28, ‡] M. Khabibullin,[26] A. Khotjantsev,[26] T. Kikawa,[32] H. Kim,[41] J. Kim,[4, 61] S. King,[44] J. Kisiel,[50] A. Knight,[65] A. Knox,[33] T. Kobayashi,[16, †] L. Koch,[53] T. Koga,[54] A. Konaka,[61] L.L. Kormos,[33] Y. Koshio,[40, ‡] K. Kowalik,[38] H. Kubo,[32] Y. Kudenko,[26, §] N. Kukita,[41] S. Kuribayashi,[32] R. Kurjata,[64] T. Kutter,[35] M. Kuze,[57] L. Labarga,[1] J. Lagoda,[38] M. Lamoureux,[24] M. Laveder,[24] M. Lawe,[33] M. Licciardi,[10] T. Lindner,[61] R.P. Litchfield,[14] S.L. Liu,[39] X. Li,[39] A. Longhin,[24] L. Ludovici,[25] X. Lu,[42] T. Lux,[18] L.N. Machado,[23] L. Magaletti,[22] K. Mahn,[36] M. Malek,[49] S. Manly,[46] L. Maret,[13] A.D. Marino,[7] J.F. Martin,[60] T. Maruyama,[16, †] T. Matsubara,[16] K. Matsushita,[54] V. Matveev,[26] K. Mavrokoridis,[34] E. Mazzucato,[6] M. McCarthy,[69] N. McCauley,[34] K.S. McFarland,[46] C. McGrew,[39] A. Mefodiev,[26] C. Metelko,[34] M. Mezzetto,[24] A. Minamino,[68] O. Mineev,[26] S. Mine,[5] M. Miura,[55, ‡] L. Molina Bueno,[11] S. Moriyama,[55, ‡] J. Morrison,[36] Th.A. Mueller,[10] L. Munteanu,[6] S. Murphy,[11] Y. Nagai,[7] T. Nakadaira,[16, †] M. Nakahata,[55, 28] Y. Nakajima,[55] A. Nakamura,[40] K.G. Nakamura,[32] K. Nakamura,[28, 16, †] S. Nakayama,[55, 28] T. Nakaya,[32, 28] K. Nakayoshi,[16, †] C. Nantais,[60] T.V. Ngoc,[20, ¶] K. Niewczas,[67] K. Nishikawa,[16, **] Y. Nishimura,[29] T.S. Nonnenmacher,[21] F. Nova,[53] P. Novella,[19] J. Nowak,[33] J.C. Nugent,[14] H.M. O'Keeffe,[33] L. O'Sullivan,[49] T. Odagawa,[32] K. Okumura,[56, 28] T. Okusawa,[41] S.M. Oser,[4, 61] R.A. Owen,[44] Y. Oyama,[16, †] V. Palladino,[23] J.L. Palomino,[39] V. Paolone,[43] W.C. Parker,[47] P. Paudyal,[34] M. Pavin,[61] D. Payne,[34] G.C. Penn,[34] L. Pickering,[36] C. Pidcott,[49] G. Pintaudi,[68] E.S. Pinzon Guerra,[69] C. Pistillo,[2] B. Popov,[52, ††] K. Porwit,[50] M. Posiadala-Zezula,[63] A. Pritchard,[34] B. Quilain,[28] T. Radermacher,[48] E. Radicioni,[22] B. Radics,[11] P.N. Ratoff,[33] E. Reinherz-Aronis,[8] C. Riccio,[23] E. Rondio,[38] S. Roth,[48] A. Rubbia,[11] A.C. Ruggeri,[23] A. Rychter,[64] K. Sakashita,[16, †] F. Sánchez,[13] C.M. Schloesser,[11] K. Scholberg,[9, ‡] J. Schwehr,[8] M. Scott,[21] Y. Seiya,[41, ‡‡] T. Sekiguchi,[16, †] H. Sekiya,[55, 28, ‡] D. Sgalaberna,[12] R. Shah,[53, 42] A. Shaikhiev,[26] F. Shaker,[66] A. Shaykina,[26] M. Shiozawa,[55, 28] W. Shorrock,[21] A. Shvartsman,[26] A. Smirnov,[26] M. Smy,[5] J.T. Sobczyk,[67] H. Sobel,[5, 28] F.J.P. Soler,[14] Y. Sonoda,[55] J. Steinmann,[48] S. Suvorov,[26, 6] A. Suzuki,[31] S.Y. Suzuki,[16, †] Y. Suzuki,[28] A.A. Sztuc,[21] M. Tada,[16, †] M. Tajima,[32] A. Takeda,[55] Y. Takeuchi,[31, 28] H.K. Tanaka,[55, ‡] H.A. Tanaka,[51, 60] S. Tanaka,[41] L.F. Thompson,[49] W. Toki,[8] C. Touramanis,[34] K.M. Tsui,[34] T. Tsukamoto,[16, †] M. Tzanov,[35] Y. Uchida,[21] W. Uno,[32] M. Vagins,[28, 5] S. Valder,[65] Z. Vallari,[39] D. Vargas,[18] G. Vasseur,[6] C. Vilela,[39] W.G.S. Vinning,[65] T. Vladisavljevic,[42, 28] V.V. Volkov,[26] T. Wachala,[15] J. Walker,[66] J.G. Walsh,[33] Y. Wang,[39] D. Wark,[53, 42] M.O. Wascko,[21] A. Weber,[53, 42] R. Wendell,[32, ‡] M.J. Wilking,[39] C. Wilkinson,[2] J.R. Wilson,[30] R.J. Wilson,[8] K. Wood,[39] C. Wret,[46] Y. Yamada,[16, **] K. Yamamoto,[41, ‡‡] C. Yanagisawa,[39, §§] G. Yang,[39] T. Yano,[55] K. Yasutome,[32] S. Yen,[61] N. Yershov,[26] M. Yokoyama,[54, ‡] T. Yoshida,[57] M. Yu,[69] A. Zalewska,[15] J. Zalipska,[38] K. Zaremba,[64] G. Zarnecki,[38] M. Ziembicki,[64] E.D. Zimmerman,[7] M. Zito,[6] S. Zsoldos,[44] and A. Zykova[26]

(The T2K Collaboration)

[1] *University Autonoma Madrid, Department of Theoretical Physics, 28049 Madrid, Spain*

[2] *University of Bern, Albert Einstein Center for Fundamental Physics, Laboratory for High Energy Physics (LHEP), Bern, Switzerland*

[3] Boston University, Department of Physics, Boston, Massachusetts, U.S.A.
[4] University of British Columbia, Department of Physics and Astronomy, Vancouver, British Columbia, Canada
[5] University of California, Irvine, Department of Physics and Astronomy, Irvine, California, U.S.A.
[6] IRFU, CEA Saclay, Gif-sur-Yvette, France
[7] University of Colorado at Boulder, Department of Physics, Boulder, Colorado, U.S.A.
[8] Colorado State University, Department of Physics, Fort Collins, Colorado, U.S.A.
[9] Duke University, Department of Physics, Durham, North Carolina, U.S.A.
[10] Ecole Polytechnique, IN2P3-CNRS, Laboratoire Leprince-Ringuet, Palaiseau, France
[11] ETH Zurich, Institute for Particle Physics and Astrophysics, Zurich, Switzerland
[12] CERN European Organization for Nuclear Research, CH-1211 Genve 23, Switzerland
[13] University of Geneva, Section de Physique, DPNC, Geneva, Switzerland
[14] University of Glasgow, School of Physics and Astronomy, Glasgow, United Kingdom
[15] H. Niewodniczanski Institute of Nuclear Physics PAN, Cracow, Poland
[16] High Energy Accelerator Research Organization (KEK), Tsukuba, Ibaraki, Japan
[17] University of Houston, Department of Physics, Houston, Texas, U.S.A.
[18] Institut de Fisica d'Altes Energies (IFAE), The Barcelona Institute of Science and Technology, Campus UAB, Bellaterra (Barcelona) Spain
[19] IFIC (CSIC & University of Valencia), Valencia, Spain
[20] Institute For Interdisciplinary Research in Science and Education (IFIRSE), ICISE, Quy Nhon, Vietnam
[21] Imperial College London, Department of Physics, London, United Kingdom
[22] INFN Sezione di Bari and Università e Politecnico di Bari, Dipartimento Interuniversitario di Fisica, Bari, Italy
[23] INFN Sezione di Napoli and Università di Napoli, Dipartimento di Fisica, Napoli, Italy
[24] INFN Sezione di Padova and Università di Padova, Dipartimento di Fisica, Padova, Italy
[25] INFN Sezione di Roma and Università di Roma "La Sapienza", Roma, Italy
[26] Institute for Nuclear Research of the Russian Academy of Sciences, Moscow, Russia
[27] International Centre of Physics, Institute of Physics (IOP), Vietnam Academy of Science and Technology (VAST), 10 Dao Tan, Ba Dinh, Hanoi, Vietnam
[28] Kavli Institute for the Physics and Mathematics of the Universe (WPI), The University of Tokyo Institutes for Advanced Study, University of Tokyo, Kashiwa, Chiba, Japan
[29] Keio University, Department of Physics, Kanagawa, Japan
[30] King's College London, Department of Physics, Strand, London WC2R 2LS, United Kingdom
[31] Kobe University, Kobe, Japan
[32] Kyoto University, Department of Physics, Kyoto, Japan
[33] Lancaster University, Physics Department, Lancaster, United Kingdom
[34] University of Liverpool, Department of Physics, Liverpool, United Kingdom
[35] Louisiana State University, Department of Physics and Astronomy, Baton Rouge, Louisiana, U.S.A.
[36] Michigan State University, Department of Physics and Astronomy, East Lansing, Michigan, U.S.A.
[37] Miyagi University of Education, Department of Physics, Sendai, Japan
[38] National Centre for Nuclear Research, Warsaw, Poland
[39] State University of New York at Stony Brook, Department of Physics and Astronomy, Stony Brook, New York, U.S.A.
[40] Okayama University, Department of Physics, Okayama, Japan
[41] Osaka City University, Department of Physics, Osaka, Japan
[42] Oxford University, Department of Physics, Oxford, United Kingdom
[43] University of Pittsburgh, Department of Physics and Astronomy, Pittsburgh, Pennsylvania, U.S.A.
[44] Queen Mary University of London, School of Physics and Astronomy, London, United Kingdom
[45] University of Regina, Department of Physics, Regina, Saskatchewan, Canada
[46] University of Rochester, Department of Physics and Astronomy, Rochester, New York, U.S.A.
[47] Royal Holloway University of London, Department of Physics, Egham, Surrey, United Kingdom
[48] RWTH Aachen University, III. Physikalisches Institut, Aachen, Germany
[49] University of Sheffield, Department of Physics and Astronomy, Sheffield, United Kingdom
[50] University of Silesia, Institute of Physics, Katowice, Poland
[51] SLAC National Accelerator Laboratory, Stanford University, Menlo Park, California, USA
[52] Sorbonne Université, Université Paris Diderot, CNRS/IN2P3, Laboratoire de Physique Nucléaire et de Hautes Energies (LPNHE), Paris, France
[53] STFC, Rutherford Appleton Laboratory, Harwell Oxford, and Daresbury Laboratory, Warrington, United Kingdom
[54] University of Tokyo, Department of Physics, Tokyo, Japan
[55] University of Tokyo, Institute for Cosmic Ray Research, Kamioka Observatory, Kamioka, Japan
[56] University of Tokyo, Institute for Cosmic Ray Research, Research Center for Cosmic Neutrinos, Kashiwa, Japan
[57] Tokyo Institute of Technology, Department of Physics, Tokyo, Japan
[58] Tokyo Metropolitan University, Department of Physics, Tokyo, Japan
[59] Tokyo University of Science, Faculty of Science and Technology, Department of Physics, Noda, Chiba, Japan
[60] University of Toronto, Department of Physics, Toronto, Ontario, Canada
[61] TRIUMF, Vancouver, British Columbia, Canada
[62] University of Victoria, Department of Physics and Astronomy, Victoria, British Columbia, Canada

[63] University of Warsaw, Faculty of Physics, Warsaw, Poland
[64] Warsaw University of Technology, Institute of Radioelectronics and Multimedia Technology, Warsaw, Poland
[65] University of Warwick, Department of Physics, Coventry, United Kingdom
[66] University of Winnipeg, Department of Physics, Winnipeg, Manitoba, Canada
[67] Wroclaw University, Faculty of Physics and Astronomy, Wroclaw, Poland
[68] Yokohama National University, Faculty of Engineering, Yokohama, Japan
[69] York University, Department of Physics and Astronomy, Toronto, Ontario, Canada
(Dated: October 11, 2019)

INTRODUCTION

The current laws of physics do not explain the observed imbalance of matter and antimatter in the universe. Sakharov proposed [1] that an explanation would require the violation of charge-conjugation parity-reversal (CP) symmetry between matter and antimatter. The only CP violation observed so far is in the weak interactions of quarks [2], and it is too small to explain the matter-antimatter imbalance of the universe. It has been shown that CP violation in the lepton sector could generate the matter-antimatter disparity through the process called leptogenesis [3]. The quantum mixing of neutrinos [4, 5], the neutral leptons in the Standard Model, provides a potential source of CP violation through a complex phase δ_{CP}, which may have consequences for theoretical models of leptogenesis [6]. This CP violation can be measured in muon neutrino to electron neutrino oscillations and the corresponding antineutrino oscillations, which are experimentally accessible with accelerator-produced beams as established by the Tokai-to-Kamioka (T2K) experiment [7]. Until now, the value of δ_{CP} has not been significantly constrained by neutrino oscillation experiments. Here the T2K collaboration reports a measurement that favors large enhancement of the neutrino oscillation probability, excluding values of δ_{CP} which result in a large enhancement of the observed anti-neutrino oscillation probability at three standard deviations (3σ). The 3σ confidence level interval for δ_{CP}, which is cyclic and repeats every 2π, is $[-3.41, -0.03]$ for the so-called normal mass ordering, and $[-2.54, -0.32]$ for the inverted mass ordering. Our results show an indication of CP violation in the lepton sector. Herein we establish methods for sensitive searches for matter-antimatter asymmetry in neutrino oscillations using accelerator-produced neutrino beams. Future measurements with larger data samples will determine whether the leptonic CP violation is larger than the quark sector CP violation.

MAIN

Previous observations of neutrino oscillations have established that the three known neutrino flavour states, ν_e, ν_μ and ν_τ are mixtures of three mass states, ν_1, ν_2 and ν_3 [8–11]. This mixing is described by a unitary matrix called the Pontecorvo-Maki-Nakagawa-Sakata (PMNS) matrix [12, 13], which can be parameterized by three mixing angles θ_{12}, θ_{13} and θ_{23}, and a complex phase, δ_{CP}. The probabilities for the neutrinos to oscillate from one flavour state to another as they travel depend on these mixing parameters and the mass squared differences ($\Delta m^2_{ij} = m^2_i - m^2_j$) between the neutrino mass states. The PMNS parameters and the mass squared differences are referred to as "oscillation parameters". It is known that ν_1 and ν_2 lie close to each other in mass, with $\Delta m^2_{21} = (7.53 \pm 0.18) \times 10^{-5}\,\mathrm{eV}^2/c^4$, while $|\Delta m^2_{32}|$ is two orders of magnitude larger. However, it is not known whether m_3 has a larger or smaller mass than m_1 and m_2 [2]. The case where the mass of m_3 is larger (smaller) is called the normal (inverted) ordering. The CP symmetry violating effect in neutrino and antineutrino oscillations has a magnitude that depends on the Jarlskog invariant:

$$J_{CP,l} = \frac{1}{8} \cos\theta_{13} \sin(2\theta_{12}) \sin(2\theta_{23}) \sin(2\theta_{13}) \sin(\delta_{CP}) \quad (1)$$

[14, 15]. According to current measurements, this is approximately $0.033 \sin(\delta_{CP})$ [2]. This value has the potential to be three orders of magnitude larger than the measured quark sector CP violation ($J_{CP,q} = 3 \times 10^{-5}$) [2]. Prior to this work, no experiment has excluded any values of δ_{CP} (taking into account both mass orderings) at the 99.73% (3σ) confidence level, considered as evidence in the particle physics community.

T2K is a long-baseline neutrino experiment that uses beams of muon neutrinos and antineutrinos, with energy spectra peaked at 0.6 GeV. We measure interactions of the neutrinos at a near detector facility 280 m from the beam production point which characterizes the beam and the interactions of the neutrinos before oscillations. The beam then propagates 295 km through the Earth to the T2K far detector, Super-Kamiokande (SK). SK measures the oscillated beam, which gives sensitivity to the oscillation parameters.

For the T2K beam energy and propagation distance, the probability for muon (anti)neutrinos to oscillate to electron (anti)neutrinos is given at leading order in δ_{CP} including the CP-violating term but neglecting effects from propagation through matter by:

$$P(\nu_\mu \to \nu_e) \approx \sin^2(2\theta_{13})\sin^2(\theta_{23})\sin^2\left(\frac{1.27\Delta m^2_{32}L}{E}\right) \mp \frac{1.27\Delta m^2_{21}L}{E} 8J_{CP}\sin^2\left(\frac{1.27\Delta m^2_{32}L}{E}\right). \quad (2)$$

Here, E is the energy of the neutrino in GeV, the mass squared differences are given in eV^2/c^4 and L is the propagation baseline in km. The second term in Eq. 2 has a negative sign for neutrinos and a positive sign for antineutrinos. The baseline and beam energy are optimised so that at T2K's baseline, the probability to oscillate to electron neutrinos reaches a maximum at energies around the T2K beam energy. While the probability of oscillation to electron neutrinos is small, muon neutrinos also oscillate to tau neutrinos, which are not identifiable at SK for T2K's beam energies. Overall, the probability for muon neutrinos and antineutrinos to maintain their initial flavour is:

$$P(\nu_\mu \to \nu_\mu) \approx 1 - 4\cos^2(\theta_{13})\sin^2(\theta_{23}) \times \left[1 - \cos^2(\theta_{13})\sin^2(\theta_{23})\right]\sin^2\left(\frac{1.27\Delta m^2_{32}L}{E}\right). \quad (3)$$

As the probability for oscillation to tau neutrinos is large at the T2K modal beam energy and baseline, there is a minimum in the muon neutrino energy spectrum. The position of this minimum gives the experiment sensitivity to the magnitude of Δm^2_{32} and the depth gives sensitivity to $\sin^2(2\theta_{23})$. The height of the peak in the electron neutrino energy spectrum at the oscillation maximum is, at leading order, determined by $\sin^2(\theta_{23})$ and $\sin^2(2\theta_{13})$ (see Eq. 2). However, it also has a sub-leading dependence on δ_{CP} and the neutrino mass ordering, giving sensitivity to these parameters. Due to this interdependence, determining the other PMNS mixing parameters is important in measuring δ_{CP}. As can be seen from Figure 1, changing δ_{CP} from $+\frac{\pi}{2}$ to $-\frac{\pi}{2}$ can lead to $\mathcal{O}(40\%)$ changes in the number of electron neutrinos expected at SK. In the T2K analysis we use the full oscillation probability including the effect of the neutrinos propagating through matter, which is a small perturbation to the probability discussed above [16].

The T2K neutrino beam is generated at the Japan Proton Accelerator Research Complex (J-PARC) by impinging a 30 GeV beam of protons onto a graphite target [17]. This interaction creates a large number of secondary hadrons, which are focused using magnetic horns. A (antineutrino-) neutrino-enhanced beam is selected by focusing (negatively-) positively-charged particles (dominantly pions), by choosing the polarity of the magnetic field produced by the horns. The beam axis is directed 2.5° away from the SK detector, taking advantage of the kinematics of the two-body pion decay to produce a narrow neutrino spectrum peaked at the expected energy of maximum oscillation probability [18]. The results reported here are based on SK data collected between 2009 and 2018 in (anti)neutrino mode and include a neutrino beam exposure of 1.49×10^{21} (1.64×10^{21}) J-PARC protons hitting the T2K neutrino production target.

Neutrinos are detected by observing the particles they produce when they interact. At neutrino energies of 0.6 GeV the dominant interaction process is Charged-Current Quasi-Elastic (CCQE) scattering via the exchange of a W boson with a single neutron or proton bound in the target nucleus. In this process the neutrino (antineutrino) turns into a charged lepton (antilepton) of the same flavour. We are thereby able to identify the incoming neutrino's flavour.

The T2K near detector facility consists of two detectors both located 280 m downstream of the beam production target [17]. The INGRID detector [19], located on the beam axis, monitors the direction and stability of the neutrino beam. The ND280 detector [20–24] is located at the same angle away from the beam axis as SK, and characterizes the rate of neutrino interactions from the beam before oscillations have occurred. ND280 is magnetized so that charged leptons and antileptons bend in opposite directions as they traverse the detector, thereby allowing the neutrino and antineutrino interaction rates in each beam mode to be measured independently. In this analysis, we select samples enriched in CCQE events and also several control samples enriched in interactions from other processes, allowing their rates to be measured separately. Here we use ND280 data that include a neutrino beam exposure of 5.8×10^{20} (3.9×10^{20}) protons hitting the T2K neutrino production target in (anti)neutrino-mode.

SK is a 50 kt water detector instrumented with photomultiplier tube light sensors [25]. In SK, Cherenkov light is produced as charged particles above a momentum threshold travel through the water. This light is emitted in ring patterns which are detected by the light sensors. Due to their lower mass, electrons scatter significantly more frequently (both elastically and inelastically) than muons so their Cherenkov rings are blurred. We use this blurring to identify the charged lepton's flavour, as illustrated in Figure 2.

We form five independent samples of SK events. For both neutrino- and antineutrino-beam mode there is a sample of events that contain a single muon-like ring, and a sample of events that contain only a single electron-like ring. These single-lepton samples are dominated by CCQE interactions. In neutrino-mode there is a sample containing an electron-like ring as well as the signature of an additional delayed electron from the decay of a charged pion and subsequent muon. We do not use this sample in antineutrino-mode because charged pions from antineutrino interactions are mostly absorbed by a nucleus before

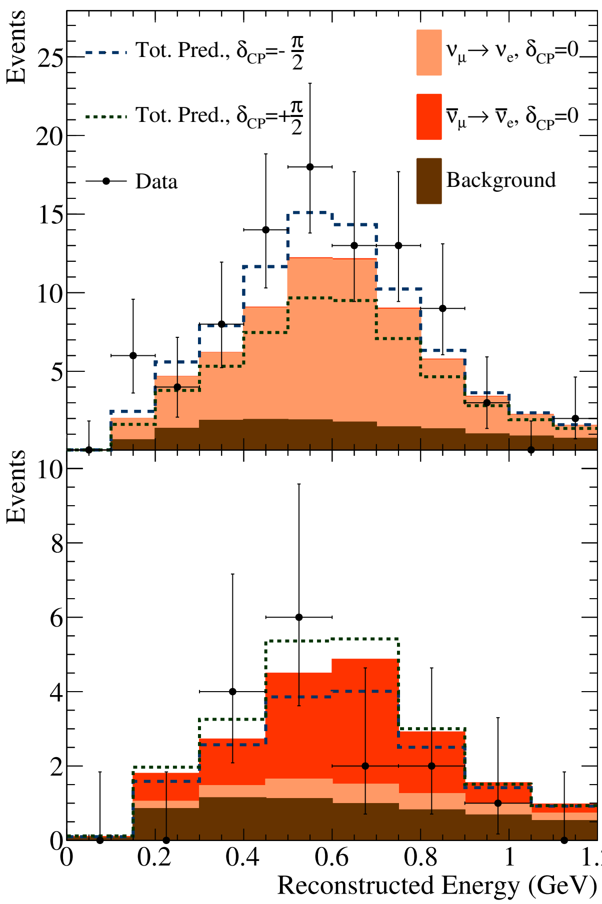

Sample	ν-mode Events	$\bar{\nu}$-mode Events
Single Electron	75 (74.8)	15 (17.2)
Charged Pion	15 (7.0)	N/A

FIG. 1. The upper (middle) panel shows the reconstructed neutrino energy spectra for the SK samples containing electron-like events in (anti)neutrino-mode beam running. The uncertainty shown around the data points accounts for statistical uncertainty. The uncertainty range is chosen to include all points for which the measured number of data events is inside the 68% confidence interval of a Poisson distribution centred at that point. The solid stacked chart shows the predicted number of events for the CP-conserving point $\delta_{CP} = 0$ separated according to whether the event was from an oscillated neutrino or antineutrino or from a background process. The dashed lines show the total predicted number of events for the two most extreme CP-violating cases. The lower table shows the measured (expected for $\delta_{CP} = -\frac{\pi}{2}$) number of events in each electron-like SK sample. For all predictions, normal ordering is assumed, and $\sin^2\theta_{23}$ and Δm^2_{32} are at their best-fit values. $\sin^2\theta_{13}$, $\sin^2\theta_{12}$ and Δm^2_{21} take the values indicated by external world average measurements [2]. The parameters accounting for systematic uncertainties take their best-fit values after the near-detector fit.

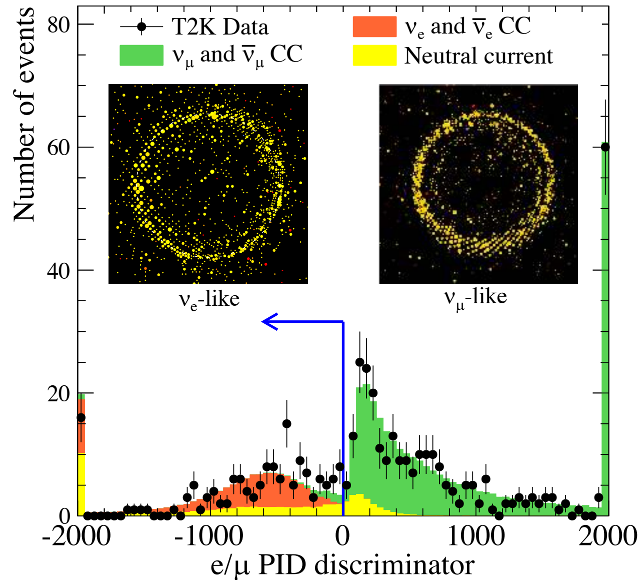

FIG. 2. Distribution of the particle identification (PID) parameter used to classify Cherenkov rings as electron-like and muon-like. Events to the left of the blue line are classified as electron-like and those to the right as muon-like. The filled histograms show the expected number of single ring events after neutrino oscillations. The PID algorithm uses properties of the light distribution such as the blurriness of the Cherenkov ring to classify events. The insets show examples of an electron-like (left) and muon-like (right) Cherenkov ring.

they decay. Identifying both muon and electron neutrino interactions in both the neutrino- and antineutrino-mode beams allows us to measure the probabilities for four oscillation channels: $\nu_\mu \rightarrow \nu_\mu$ and $\bar{\nu}_\mu \rightarrow \bar{\nu}_\mu$, $\nu_\mu \rightarrow \nu_e$ and $\bar{\nu}_\mu \rightarrow \bar{\nu}_e$.

We define a model of the expected number of neutrino events as a function of kinematic variables measured in our detectors with degrees of freedom for each of the oscillation parameters and for each source of systematic uncertainty. Systematic uncertainties arise in the modeling of neutrino-nucleus interactions in the detector, the modeling of the neutrino production, and the modeling of the detector's response to neutrino interaction products. Where possible, we constrain the model using external data. For example, the solar oscillation parameters, Δm^2_{21} and $\sin^2(\theta_{12})$, which T2K is not able to measure, are constrained using world average data [2]. Whilst we are sensitive to $\sin^2\theta_{13}$, we use the combination of measurements from the Daya Bay, RENO and Double Chooz reactor experiments to constrain this parameter [2], as they make a much more precise measurement than using T2K data alone (see upper panel of Figure 3). We measure the oscillation parameters by doing a marginal likelihood fit of this model to our near and far detector data. We perform several analyses using both Bayesian and frequentist statistical paradigms. Exclusive measurements of (anti)neutrino candidates in the near detector, one of which is shown in Figure 4, strongly constrain the neutrino production and interaction models, reducing the uncertainty on the predicted number of events in the four single-lepton SK samples from 13-17% to 4-9%, depending on the sample. The electron-like with additional charged pion sample's uncertainty is reduced from 22% to 19%.

A neutrino's oscillation probability depends on its energy, as shown in Eqs. 2 and 3. While the energy distribution of the T2K neutrino beam is well understood, we cannot directly measure the energy of each incoming neutrino. Instead the neutrino's energy must be inferred from the momentum and direction of the charged lepton that results from the interaction. This inference relies on the correct modeling of the nuclear physics of neutrino-nucleus interactions. Modeling the strong nuclear force in multi-body problems at these energies is not computationally tractable, so approximate theories are used [26–29]. The potential biases introduced by approximations in these theories constitute the largest sources of systematic uncertainties in this measurement. Furthermore, as well as CCQE interactions, there are non-negligible contributions from interactions where additional particles are present in the final state but were not detected by T2K's detectors. To check for bias from incorrect modeling of neutrino-nucleus interactions, we performed fits to simulated data sets generated assuming a range of different models of neutrino interactions [27, 28]. We compared the measurements of the oscillation parameters obtained from these fits with the measurement from a fit to simulated data generated assuming our default model. We observed no significant biases in the obtained δ_{CP} best-fit values or changes in the interval sizes from any model tested. Any biases seen in the other oscillation parameters are incorporated as additional sources of error in the analysis.

The observed number of events at SK can be seen in Figure 1. The probability to observe an excess over prediction in one of our five samples at least as large as that seen in the electron-like charged pion sample is 6.9% for the best-fit value of the oscillation parameters. We find the data shows a preference for the normal mass ordering with a posterior probability of 89%, giving a Bayes factor of 8. We find $\sin^2(\theta_{23}) = 0.53^{+0.03}_{-0.04}$ for both mass orderings. Assuming the normal (inverted) mass ordering we find $\Delta m^2_{32} = (2.45 \pm 0.07) \times 10^{-3}$ ($\Delta m^2_{13} = (2.43 \pm 0.07) \times 10^{-3}$) eV$^2/c^4$. For δ_{CP} our best-fit value and 68% (1σ) uncertainties assuming the normal (inverted) mass ordering are $-1.89^{+0.70}_{-0.58}(-1.38^{+0.48}_{-0.54})$, with statistical uncertainty dominating. Our data show a preference for values of δ_{CP} which are near maximal CP violation (see Figure 3), while both CP conserving points, $\delta_{CP} = 0$ and $\delta_{CP} = \pi$, are ruled out at the 95% confidence level, consistent with the previous T2K measurement [8]. Here, we also produce 99.73% (3σ) confidence and credible intervals on δ_{CP}. In the normal ordering the interval contains $[-3.41,-0.03]$ (excluding 46% of the range of parameter space), while in the inverted ordering the interval contains [-2.54,-0.32] (excluding 65% of the parameter space). The 99.73% credible interval marginalized across both mass order-

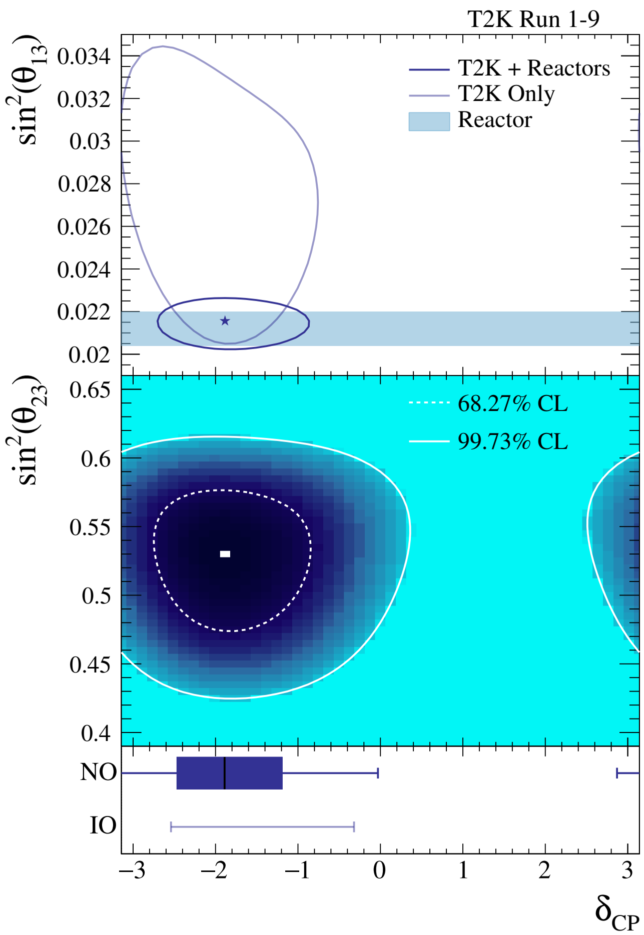

FIG. 3. The upper panel shows 2D confidence intervals at the 68.27% confidence level for δ_{CP} vs $\sin^2\theta_{13}$ in the normal ordering. The intervals labelled T2K only indicate the measurement obtained without using the external constraint on $\sin^2\theta_{13}$, while the T2K + Reactor intervals do use the external constraint. The star shows the best-fit point of the T2K + Reactors fit in the preferred normal mass ordering. The middle panel shows 2D confidence intervals at the 68.27% and 99.73% confidence level for δ_{CP} vs $\sin^2\theta_{23}$ from the T2K + Reactors fit in the normal ordering, with the colour scale representing the value of the likelihood for each parameter value. The lower panel shows 1D confidence intervals on δ_{CP} from the T2K + Reactors fit in both the normal (NO) and inverted (IO) orderings. The vertical line in the shaded box shows the best-fit value of δ_{CP}, the shaded box itself shows the 68.27% confidence interval, and the error bar shows the 99.73% confidence interval. It is notable that there are no values in the inverted ordering inside the 68.27% interval.

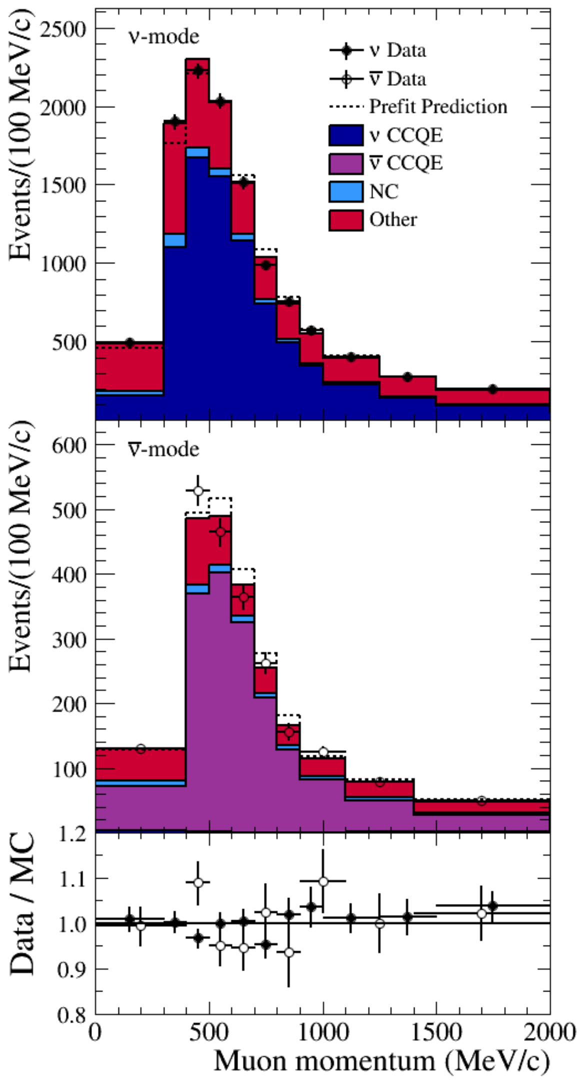

FIG. 4. Reconstructed muon momentum in two of the ND280 CCQE-like event samples for both neutrino (top) and antineutrino (middle) beam mode. The prediction with all parameters set to their best-fit value from a fit to the ND280 data is shown by the coloured histograms, split into true neutrino CCQE, antineutrino CCQE, neutral current (NC) and all other interactions. The dashed line shows the prediction before a fit to the ND280 data. The bottom panel shows the ratio of the observed data to the best-fit prediction (MC) in both neutrino and antineutrino mode samples.

ings contains [-3.48,0.13] (excluding 42% of the parameter space). The CP-conserving points are not both excluded at the 99.73% level. However, this is the first time closed 99.73% (3σ) intervals on the CP-violating phase δ_{CP} have been reported (taking into account both mass orderings) and a large range of values around $+\pi/2$ are excluded.

We thank the J-PARC staff for superb accelerator performance. We thank the CERN NA61/SHINE Collaboration for providing valuable particle production data. We acknowledge the support of MEXT, Japan; NSERC (Grant No. SAPPJ-2014-00031), NRC and CFI, Canada; CEA and CNRS/IN2P3, France; DFG, Germany; INFN, Italy; National Science Centre (NCN) and Ministry of Science and Higher Education, Poland; RSF (Grant # 19-12-00325) and Ministry of Science and Higher Education, Russia; MINECO and ERDF funds, Spain; SNSF and SERI, Switzerland; STFC, UK; and DOE, USA. We also thank CERN for the UA1/NOMAD magnet, DESY for the HERA-B magnet mover system, NII for SINET4, the WestGrid, SciNet and CalculQuebec consortia in Compute Canada, and GridPP in the United Kingdom. In addition, participation of individual researchers and institutions has been further supported by funds from ERC (FP7), H2020 Grant No. RISE-GA644294-JENNIFER, EU; JSPS, Japan; Royal Society, UK; the DOE Early Career program, USA.

METHODS

Neutrino Production Modeling

The predicted neutrino and antineutrino fluxes, including the energies and flavours of (anti)neutrinos, are estimated using a detailed simulation of the T2K beam line. Measurement of the proton beam orbit, transverse width and divergence, and intensity are used as the initial conditions before simulating the interactions of protons in the T2K target to produce the secondary particles that decay to neutrinos. Particle interactions and production inside the target are simulated with FLUKA2011 [30, 31], while particle propagation outside of the target is simulated with GEANT3 [32]. Interaction rates and hadron production in the simulation are tuned with hadron interaction data from external experiments, primarily the NA61/SHINE experiment which has collected data for T2K at the J-PARC proton beam energy of 30 GeV with the T2K target material of graphite [33]. Measurements of the magnetic horns' currents during beam operation and of the horns' magnetic fields before installation ensure accurate modeling of the charged particle focusing in the flux simulation. The simulated fluxes are used as inputs to simulations of neutrino interactions and particle detection in the ND280 and SK detectors. The spectrum of muon (anti)neutrinos produced from the decays of focused charged pions peaks at an energy of 0.6 GeV for an off-axis angle of 2.5°. Near the peak energy, 97.2% (96.2%) of the (anti)neutrino-mode beam is initially ν_μ ($\bar{\nu}_\mu$). The remaining components are mostly $\bar{\nu}_\mu$ (ν_μ); contaminations of $\nu_e + \bar{\nu}_e$ are only 0.47% (0.49%).

The uncertainty on the flux calculation is evaluated by propagating uncertainties on the proton beam measurements, hadronic interactions, material modeling and alignment of beam line elements, and horn current and field measurements. In each case, variations of the source of uncertainty are considered and the effect on the flux simulation is evaluated. The INGRID on-axis neutrino detector is not used to tune the beam direction during operation. Hence, it provides an independent measurement of the beam direction [34], which is used to validate the flux simulation. The uncertainty on the INGRID beam direction measurement is propagated in the flux model. The variations are used to calculate covariances for the flux prediction in bins of energy, flavour, neutrino/antineutrino mode and detector (ND280 and SK). These covariances are used to propagate uncertainties on the flux prediction in the oscillation analysis. The dominant source of systematic uncertainty is from the hadron interaction data and models. The uncertainty on the flux normalization near the peak energy of 0.6 GeV is 9%. Uncertainties on the proton beam orbit and alignment of beam line elements correspond to an uncertainty on the off-axis angle at the ND280 and SK detectors, corresponding to uncertainties on the peak energy of the neutrino spectrum at those detectors.

Neutrino Interaction Modeling

The T2K detectors measure products of neutrinos and antineutrinos interacting on nuclei and free protons with energies ranging from ∼0.1 GeV to 30 GeV. These interactions are modeled with the NEUT [35] neutrino interaction generator, using version 5.3.2. NEUT uses a range of models to describe the physics of the initial nuclear state, the neutrino-nucleon(s) interaction, and the interactions of final state particles in the nuclear medium. The primary signal processes in SK are defined by the presence of a single charged lepton candidate with no other visible particles. The dominant process at the peak energy of 0.6 GeV is Charged-Current Quasi-Elastic (CCQE) scattering. This process corresponds to the neutrino or antineutrino scattering on a single nucleon bound in the target nucleus. The neutrino-nucleon scattering in NEUT is implemented in the formalism of Llewellyn-Smith [36]. For the initial nuclear state, NEUT implements a relativistic Fermi gas (RFG) model of the target nucleus, including long-range correlations evaluated using the random phase approximation (RPA) [37]. NEUT includes an alternative initial state model based on spectral functions describing the initial momentum and removal energy for bound nucleons [38].

Additional processes that can produce a signal-like final state are modeled in NEUT. The 2p-2h model of Nieves *et al.* [39, 40] predicts production of multinucleon excitations, where more than one nucleon and no pions are ejected in the final state. The ejected nucleons are typically below detection threshold in a water Cherenkov detector, making this process indistinguishable from the CCQE process.

The signal candidate sample with one prompt electron-like ring and the presence of an electron from muon decay consists primarily of interactions where a pion is produced. These single-pion interactions can also populate the samples without an additional electron from muon decay if the pion is absorbed in the target nucleus or on a nucleus in the detector, or if it is not detected. Processes producing a single pion and one nucleon are described by the Rein-Sehgal model [41]. Processes with multiple pions are simulated with a custom model below 2 GeV of hadronic invariant mass and by PYTHIA [42] otherwise. These processes may be selected as events with single Cherenkov rings if the pion is absorbed in the target nucleus or surrounding nuclei, or if it is not detected. The final state interactions of pions and protons in the target nucleus are modeled with the NEUT intranuclear cascade model where the density dependence of the mean free path for pions in the target nucleus is calculated based on the Δ-hole model of Oset *et. al.* [43] at low momenta and from p-π scattering data from the SAID database at high momenta. The microscopic interaction rates for exclusive pion scattering modes are then tuned to macroscopic π-nucleus scattering data.

We consider two types of systematic uncertainties on neutrino interaction modeling in the oscillation measurement. In the first, parameters in the nominal interaction model are allowed to vary and are constrained by ND280 data. These parameters are then marginalized over when measuring oscillation parameters. They include uncertainties on nucleon form factors, the corrections for long-range correlations, the rates of different neutrino interaction processes, the final state kinematics of the CCQE, 2p-2h and single pion production processes, and the rates of pion final state interactions. Most of these are parameters in the models with physical interpretations, and they modify the overall rate of interactions, the final state topology, and the kinematics of final state particles. We also include an uncertainty on the ν_e and $\bar{\nu}_e$ cross sections relative to the ν_μ and $\bar{\nu}_\mu$ cross sections. This introduces a direct uncertainty on the relative prediction of ν_e and $\bar{\nu}_e$ candidates, and is motivated by uncertainties in the neutrino-nucleon scattering cross section arising from the charged lepton masses [44]. The second type of systematic uncertainty is evaluated by introducing simulated data generated with an alternative model into the analysis and evaluating the impact on measured oscillation parameters. This approach is used to evaluate the effect of changes to the nuclear initial state model including the use of the spectral functions, and changes to removal energy for initial state nucleons. This approach is also applied to evaluate the impact of changes to the 2p-2h interaction cross section as a function of energy, sensitivity to an alternative single pion production model [45, 46], and sensitivity to alternative multi-pion production tuning [47].

Super-Kamiokande Event Reconstruction

Photosensors installed on the SK inner detector register Cherenkov light produced as charged particles produced by neutrino interactions travel through the water volume [25]. Photosensor activity clustered in time, on the order of a micro-second, is called an event. Events coincident with the T2K-beam timing are selected as candidate beam neutrino interactions.

Neutrino interaction events in SK often have multiple periods of photosensor activity separated in time within an event. The most frequent example is a muon decaying into an electron. A decay electron can be used to tag a muon even when the muon energy is below the Cherenkov threshold, e.g. the case that the muon is produced by a charged pion decaying at rest. Such sub-events are searched for with a peak finding algorithm and reconstructed separately in later processes.

The kinematics of the charged particles are reconstructed from the timing and the number of detected photons of each photosensor signal by using a maximum likelihood algorithm [48]. The likelihood consists of the probability of each photosensor to detect photons or not and the charge and timing probability density functions of the hit photosensors. This new reconstruction algorithm makes use of the timing and charge information obtained by all the photosensors simultaneously, which leads to better kinematic resolutions and particle classifying performances compared to the previously used reconstruction algorithm.

The five signal samples are formed by using the reconstructed event kinematics. All the selected events are required to have little photosensor activity in an outer veto detector, and the reconstructed neutrino interaction position is required to be inside the inner detector fiducial volume. The reconstruction improvement enabled us to extend the fiducial volumes used in the analysis. We performed a dedicated study to optimize the fiducial volume to maximize T2K sensitivities to oscillation parameters taking into account both the statistical and systematical uncertainties. The position dependent SK detector systematics are estimated by using SK atmospheric neutrino interaction events. The fiducial volume expansion contributes to the increase of selected electron-like (muon-like) events by 25% (14%) [49].

Systematic uncertainties regarding SK detector modeling were evaluated by using cosmic muon and atmospheric neutrino events observed at SK. Uncertainties on Cherenkov ring counting and particle identification are evaluated by using events from atmospheric neutrino interactions. Errors on absolute energy scale, tagging efficiency of decay electrons, and position reconstruction bias are estimated by using non-neutrino events.

Statistical Methods

We use a binned likelihood-ratio method comparing the observed and predicted numbers of muon- and electron-neutrino candidate events in our five samples. In neutrino beam mode these are electron-like, muon-like and electron-like charged pion samples, while in antineutrino beam mode these are electron-like and muon-like samples. The samples are binned in reconstructed energy and, for the electron-neutrino-like samples, the angle between the lepton and the beam direction. In particular, best-fits are determined by minimising the sum of the following likelihood function (marginalized over nuisance parameters) over all of our samples

$$-2\ln\lambda(\overline{\delta_{CP}};\mathbf{a}) = 2\sum_{i=1}^{N}\left[n_i^{obs}\ln\left(\frac{n_i^{obs}}{n_i^{exp}}\right)+n_i^{exp}-n_i^{obs}\right] + (\mathbf{a}-\mathbf{a_0})^T\mathbf{C^{-1}}(\mathbf{a}-\mathbf{a_0}) \quad (4)$$

where $\overline{\delta_{CP}}$ is the estimated value of δ_{CP}, $\mathbf{a}$ is the vector of systematic parameter values (including the remaining oscillation parameters), $\mathbf{a_0}$ is the vector of default values of the systematic parameters, $\mathbf{C}$ is the systematic parameter covariance matrix, N is the number of reconstructed energy and lepton angle bins, n_i^{obs} is the number of events observed in bin i and $n_i^{exp} = n_i^{exp}(\overline{\delta_{CP}};\mathbf{a})$ is the corresponding expected number of events. Systematic parameters are marginalized according to their prior constraints from the fit to ND280 data.

We perform both frequentist and Bayesian analyses of our data. The measurement of δ_{CP} from each of the analyses is in agreement, with the presented confidence intervals coming from a frequentist analysis and the Bayes factors and credible intervals coming from a Bayesian analysis. In the frequentist analysis a fit is first performed to the near detector samples binned in the momentum and cosine of the angle between the lepton and the beam direction, with penalty terms for flux, cross-section and detector systematic parameters at the near detector. Systematic parameter constraints are then propagated from the near to the far detector via the covariance matrix, $\mathbf{C}$, in Eq. 4 and their fitted values. The matrix is the combination of the posterior covariance from the near detector fit with the priors for the oscillation parameters, with some parameters affecting both detectors directly, while others that affect only the far detector are constrained through their correlation with near detector affecting parameters. Gaussian priors for $\sin^2(\theta_{13})$, $\sin^2(\theta_{12})$, and Δm^2_{21} are taken from the Particle Data Group's (PDG) world combinations [50], while $\sin^2(\theta_{23})$ and Δm^2_{32} (Δm^2_{13}) have uniform priors in normal (inverted) mass ordering. For the Bayesian analyses the prior for δ_{CP} is uniform, with an additional check applying a uniform prior in $\sin(\delta_{CP})$ producing the same conclusions. Furthermore, rather than fitting the near detector and propagating to the far detector as a two step process, the Bayesian analysis directly includes the near detector samples in its expression for the likelihood and therefore performs a simultaneous fit of the near and far detector data.

The neutrino oscillation probability depends non-linearly on the oscillation parameters, with different possible values of δ_{CP} corresponding to a bounded enhancement or suppression of the electron (anti)neutrino appearance probability. If statistical fluctuations in the data exceed these bounds they are not accommodated by the model, and as a result the critical $\Delta\chi^2$ value for a given confidence level is often different from the asymptotic rule of Wilks [51]. To address this problem the frequentist analysis constructs Neyman confidence intervals using the approach described by Feldman and Cousins [52] and thus critical values of $\Delta\chi^2$ vary as a function of δ_{CP} and the mass ordering. The critical values at a given confidence level are determined by fitting at least 20,000 simulated datasets for each given true value of δ_{CP} and the mass ordering. The remaining oscillation parameters are varied according to their priors. In particular, for $\sin^2(\theta_{13})$, $\sin^2(\theta_{12})$, and Δm^2_{21} these priors are taken from the PDG [50], with $\sin^2(\theta_{13})$ determined by the reactor experiments noted in the main text. For $\sin^2(\theta_{23})$, and Δm^2_{32} (Δm^2_{13}) the priors take the form of likelihood surfaces produced from fits of simulated datasets. The simulated datasets are generated using oscillation parameter best-fits in normal and inverted mass orderings. The remaining systematic parameters are varied according to their prior constraints from the fit to ND280 data.

The Bayesian analysis uses Markov Chain Monte Carlo (MCMC) to take random samples from the likelihood. The particular MCMC algorithm used is Metropolis-Hastings [53]. For a sufficiently large number of samples the Markov chain achieves an equilibrium probability distribution. The number of steps in the chain with a particular value of a parameter is proportional to the posterior probability for the parameter to have that value marginalized over all the other parameters. Credible intervals are then formed on the basis of highest posterior density, with bins of equal width in the parameter under study. Given the arbitrary initial state of the Markov chain, a finite number of samples must be obtained to allow the chain to converge to a state in which it is correctly sampling from the distribution. These preliminary 'burn-in' samples are discarded.

DATA AVAILABILITY

The likelihood surface data that support these findings will be made available for public access on http://t2k-experiment.org.

---

* now at CERN
† also at J-PARC, Tokai, Japan
‡ affiliated member at Kavli IPMU (WPI), the University of Tokyo, Japan
§ also at National Research Nuclear University "MEPhI" and Moscow Institute of Physics and Technology, Moscow, Russia
¶ also at the Graduate University of Science and Technology, Vietnam Academy of Science and Technology
** deceased
†† also at JINR, Dubna, Russia
‡‡ also at Nambu Yoichiro Institute of Theoretical and Experimental Physics (NITEP)
§§ also at BMCC/CUNY, Science Department, New York, New York, U.S.A.

[1] A. D. Sakharov, "Violation of CP Invariance, C asymmetry, and baryon asymmetry of the universe," *Pis'ma Zh. Eksp. Teor. Fiz.*, vol. 5, pp. 32–35, 1967. [Sov. Phys. Usp. 34,no.5,392-393(1991)].

[2] M. Tanabashi *et al.*, "Review of Particle Physics," *Phys. Rev.*, vol. D98, no. 3, p. 030001, 2018.

[3] M. Fukugita and T. Yanagida, "Baryogenesis Without Grand Unification," *Phys. Lett.*, vol. B174, pp. 45–47, 1986.

[4] Y. Fukuda *et al.*, "Evidence for oscillation of atmospheric neutrinos," *Phys. Rev. Lett.*, vol. 81, pp. 1562–1567, 1998.

[5] Q. R. Ahmad *et al.*, "Direct evidence for neutrino flavor transformation from neutral current interactions in the Sudbury Neutrino Observatory," *Phys. Rev. Lett.*, vol. 89, p. 011301, 2002.

[6] R. N. Mohapatra *et al.*, "Theory of neutrinos: A White paper," *Rept. Prog. Phys.*, vol. 70, pp. 1757–1867, 2007.

[7] K. Abe *et al.*, "Observation of Electron Neutrino Appearance in a Muon Neutrino Beam," *Phys. Rev. Lett.*, vol. 112, p. 061802, 2014.

[8] K. Abe *et al.*, "Search for CP Violation in Neutrino and Antineutrino Oscillations by the T2K Experiment with 2.2×10^{21} Protons on Target," *Phys. Rev. Lett.*, vol. 121, no. 17, p. 171802, 2018.

[9] S. Abe *et al.*, "Precision Measurement of Neutrino Oscillation Parameters with KamLAND," *Phys. Rev. Lett.*, vol. 100, p. 221803, 2008.

[10] D. Adey *et al.*, "Measurement of the Electron Antineutrino Oscillation with 1958 Days of Operation at Daya Bay," *Phys. Rev. Lett.*, vol. 121, no. 24, p. 241805, 2018.

[11] B. Aharmim *et al.*, "Combined Analysis of all Three Phases of Solar Neutrino Data from the Sudbury Neutrino Observatory," *Phys. Rev.*, vol. C88, p. 025501, 2013.

[12] Z. Maki, M. Nakagawa, and S. Sakata, "Remarks on the unified model of elementary particles," *Prog. Theor. Phys.*, vol. 28, pp. 870–880, 1962.

[13] B. Pontecorvo, "Neutrino Experiments and the Problem of Conservation of Leptonic Charge," *Sov. Phys. JETP*, vol. 26, pp. 984–988, 1968. [Zh. Eksp. Teor. Fiz.53,1717(1967)].

[14] P. I. Krastev and S. T. Petcov, "Resonance Amplification and t Violation Effects in Three Neutrino Oscillations in the Earth," *Phys. Lett.*, vol. B205, pp. 84–92, 1988.

[15] C. Jarlskog, "A Basis Independent Formulation of the Connection Between Quark Mass Matrices, CP Violation

and Experiment," *Z. Phys.*, vol. C29, pp. 491–497, 1985.
[16] V. Barger, K. Whisnant, S. Pakvasa, and R. J. N. Phillips, "Matter effects on three-neutrino oscillations," *Phys. Rev. D*, vol. 22, pp. 2718–2726, Dec 1980.
[17] K. Abe *et al.*, "The T2K Experiment," *Nucl. Instrum. Meth.*, vol. A659, pp. 106–135, 2011.
[18] D. Beavis, A. Carroll, I. Chiang, and E889 Collaboration, "Long baseline neutrino oscillation experiment at the ags. physics design report," 4 1995.
[19] M. Otani *et al.*, "Design and construction of INGRID neutrino beam monitor for T2K neutrino experiment," *Nucl. Instrum. Meth.*, vol. A623, pp. 368–370, 2010.
[20] P. A. Amaudruz *et al.*, "The T2K Fine-Grained Detectors," *Nucl. Instrum. Meth.*, vol. A696, pp. 1–31, 2012.
[21] S. Assylbekov *et al.*, "The T2K ND280 Off-Axis Pi-Zero Detector," *Nucl. Instrum. Meth.*, vol. A686, pp. 48–63, 2012.
[22] N. Abgrall *et al.*, "Time Projection Chambers for the T2K Near Detectors," *Nucl. Instrum. Meth.*, vol. A637, pp. 25–46, 2011.
[23] D. Allan *et al.*, "The Electromagnetic Calorimeter for the T2K Near Detector ND280," *JINST*, vol. 8, p. P10019, 2013.
[24] S. Aoki *et al.*, "The T2K Side Muon Range Detector (SMRD)," *Nucl. Instrum. Meth.*, vol. A698, pp. 135–146, 2013.
[25] Y. Fukuda *et al.*, "The Super-Kamiokande detector," *Nucl. Instrum. Meth.*, vol. A501, pp. 418–462, 2003.
[26] J. Nieves, M. Valverde, and M. J. Vicente Vacas, "Inclusive nucleon emission induced by quasi-elastic neutrino-nucleus interactions," *Phys. Rev.*, vol. C73, p. 025504, 2006.
[27] M. Martini, M. Ericson, G. Chanfray, and J. Marteau, "A Unified approach for nucleon knock-out, coherent and incoherent pion production in neutrino interactions with nuclei," *Phys. Rev.*, vol. C80, p. 065501, 2009.
[28] O. Benhar, N. Farina, H. Nakamura, M. Sakuda, and R. Seki, "Electron- and neutrino-nucleus scattering in the impulse approximation regime," *Phys. Rev.*, vol. D72, p. 053005, 2005.
[29] L. L. Salcedo, E. Oset, M. J. Vicente-Vacas, and C. Garcia-Recio, "Computer Simulation of Inclusive Pion Nuclear Reactions," *Nucl. Phys.*, vol. A484, pp. 557–592, 1988.
[30] T. Bhlen, F. Cerutti, M. Chin, A. Fass, A. Ferrari, P. Ortega, A. Mairani, P. Sala, G. Smirnov, and V. Vlachoudis, "The fluka code: Developments and challenges for high energy and medical applications," *Nuclear Data Sheets*, vol. 120, pp. 211 – 214, 2014.
[31] A. Ferrari, P. R. Sala, A. Fasso, and J. Ranft, "FLUKA: A multi-particle transport code (Program version 2005)," 2005.
[32] R. Brun, F. Bruyant, F. Carminati, S. Giani, M. Maire, A. McPherson, G. Patrick, and L. Urban, "GEANT Detector Description and Simulation Tool," 1994.
[33] N. Abgrall *et al.*, "Measurements of $\pi^{\pm}$, $K^{\pm}$, K^0_S , Λ and proton production in protoncarbon interactions at 31 GeV/c with the NA61/SHINE spectrometer at the CERN SPS," *Eur. Phys. J.*, vol. C76, no. 2, p. 84, 2016.
[34] K. Abe *et al.*, "Measurements of the T2K neutrino beam properties using the INGRID on-axis near detector," *Nucl. Instrum. Meth.*, vol. A694, pp. 211–223, 2012.
[35] Y. Hayato, "A Neutrino Interaction Simulation Program Library NEUT," *Acta Physica Polonica B*, vol. 40, p. 2477, Sep 2009.
[36] C. H. Llewellyn Smith, "Neutrino Reactions at Accelerator Energies," *Phys. Rept.*, vol. 3, pp. 261–379, 1972.
[37] J. Nieves, J. E. Amaro, and M. Valverde, "Inclusive quasielastic charged-current neutrino-nucleus reactions," *Phys. Rev. C*, vol. 70, p. 055503, Nov 2004.
J. Nieves, J. E. Amaro, and M. Valverde, "Erratum: Inclusive quasielastic charged-current neutrino-nucleus reactions [phys. rev. c 70, 055503 (2004)]," *Phys. Rev. C*, vol. 72, p. 019902, Jul 2005.
[38] O. Benhar and A. Fabrocini, "Two nucleon spectral function in infinite nuclear matter," *Phys. Rev.*, vol. C62, p. 034304, 2000.
[39] J. Nieves, I. R. Simo, and M. J. V. Vacas, "Inclusive charged-current neutrino-nucleus reactions," *Phys. Rev. C*, vol. 83, p. 045501, Apr 2011.
[40] R. Gran, J. Nieves, F. Sanchez, and M. J. Vicente Vacas, "Neutrino-nucleus quasi-elastic and 2p2h interactions up to 10 GeV," *Phys. Rev.*, vol. D88, no. 11, p. 113007, 2013.
[41] D. Rein and L. M. Sehgal, "Neutrino-excitation of baryon resonances and single pion production," *Annals of Physics*, vol. 133, no. 1, pp. 79–153, 1981.
[42] T. Sjostrand, "High-energy physics event generation with PYTHIA 5.7 and JETSET 7.4," *Comput. Phys. Commun.*, vol. 82, pp. 74–90, 1994.
[43] E. Oset, L. L. Salcedo, and D. Strottman, "A Theoretical Approach to Pion Nuclear Reactions in the Resonance Region," *Phys. Lett.*, vol. 165B, pp. 13–18, 1985.
[44] M. Day and K. S. McFarland, "Differences in quasi-elastic cross sections of muon and electron neutrinos," *Phys. Rev.*, vol. D86, p. 053003, 2012.
[45] D. Rein, "Angular Distribution in Neutrino Induced Single Pion Production Processes," *Z. Phys.*, vol. C35, pp. 43–64, 1987.
[46] M. Kabirnezhad, "Single Pion Production in Neutrino-Nucleon Interactions," *Phys. Rev.*, vol. D97, no. 1, p. 013002, 2018.
[47] T. Yang, C. Andreopoulos, H. Gallagher, K. Hoffmann, and P. Kehayias, "A Hadronization Model for Few-GeV Neutrino Interactions," *Eur. Phys. J.*, vol. C63, pp. 1–10, 2009.
[48] M. Jiang *et al.*, "Atmospheric Neutrino Oscillation Analysis With Improved Event Reconstruction in Super-Kamiokande IV," *PTEP*, vol. 2019, no. 5, p. 053F01, 2019.
[49] K. Abe, "Search for *cp* violation in neutrino and antineutrino oscillations by the t2k experiment with 2.2×10^{21} protons on target," *Phys. Rev. Lett.*, vol. 121, p. 171802, Oct 2018.
[50] M. Tanabashi *et al.*, "Review of Particle Physics," *Physical Review D*, vol. 98, p. 030001, aug 2018.
[51] S. S. Wilks, "The Large-Sample Distribution of the Likelihood Ratio for Testing Composite Hypotheses," *The Annals of Mathematical Statistics*, vol. 9, pp. 60–62, 1938.
[52] G. J. Feldman and R. D. Cousins, "A Unified approach to the classical statistical analysis of small signals," *Phys. Rev.*, vol. D57, pp. 3873–3889, 1998.
[53] W. K. Hastings, "Monte Carlo sampling methods using Markov chains and their applications," *Biometrika*, vol. 57, pp. 97–109, apr 1970.